Soft tissue tumors: perfusion and diffusion-weighted MR imaging

Rijswijk, Catharina van

Chapter 6

Diffusion-weighted MRI in the characterization of soft tissue tumors

Catharina S.P. van Rijswijk, Patrik Kunz, Pancras C.W. Hogendoorn,

Anthonie H.M. Taminiau, Joost Doornbos, Johan L. Bloem

ABSTRACT

PURPOSE:

To explore the potential of perfusion-corrected diffusion-weighted magnetic resonance (MR) imaging in characterizing soft tissue tumors.

MATERIALS AND METHODS:

Diffusion-weighted MR imaging was performed in 23 histologically proven soft tissue masses using a diffusion-weighted spin-echo sequence with diffusion gradient strengths yielding five b-values (0-701 seconds/mm^2). True diffusion coefficients and perfusion fractions were estimated and compared with apparent diffusion coefficients (ADCs).

RESULTS:

ADC values of all tumors, subcutaneous fat and muscle were significantly higher than true diffusion coefficients, indicating a contribution of perfusion to the ADC. True diffusion coefficients of malignant tumors (1.08 x 10^{-3} mm^2/second) were significantly lower than those of benign masses (1.71 x 10^{-3} mm^2/second), whereas ADC values between these groups were not significantly different.

CONCLUSION:

Perfusion-corrected diffusion-weighted MR imaging has potential in differentiating benign from malignant soft tissue masses.

INTRODUCTION

Diffusion-weighted magnetic resonance (MR) imaging reflects intravoxel incoherent motion (IVIM). In biological tissues, motion includes Brownian motion of extra-, intra- and transcellular individual water molecules (true diffusion) as well as microcirculation of blood (perfusion) (1). Both true diffusion and perfusion contribute to the frequently used apparent diffusion coefficient (ADC).

Diffusion-weighted MR imaging has been used successfully in the central nervous system (CNS), especially in the diagnosis of acute stroke (2-4), but also in distinguishing different components of brain tumors (5;6). Diffusion measurements of tumors outside the brain have also been reported. A study of osteogenic sarcoma in rats by Lang et al. indicates that diffusion-weighted MR imaging can accurately differentiate between viable and necrotic tumor regions (7). Maier et al. reported quantitative diffusion measurements of breast tumors in mice (8). Moreover, Bauer et al. reported diffusion measurements in human spine that could reliable differentiate acute benign from neoplastic vertebral compression fractures (9). These studies have

demonstrated potential for providing information that can contribute in the differentiation between benign and malignant tumors, and can identify various tumor components.

The purpose of our study was to explore the potential of true diffusion measurements, which are corrected for the perfusion effect, as a method to differentiate benign from malignant soft tissue masses.

MATERIALS AND METHODS

Patients

Between December 1999 and December 2000, we prospectively included 22 consecutive patients (11 women, 11 men; age range 11-70 years; median age 41 years) with 23 soft tissue masses, clinically suspected to be neoplasm. In all patients diagnosis was confirmed after MR imaging with histologic biopsy and/or examination of the resected specimens. Twelve masses were benign: there were two schwannomas, two patients with aggressive fibromatosis and one patient each with myositis ossificans, complex synovial cyst, vascular malformation, pigmented villonodular synovitis, ganglion, myxoma, hematoma and leiomyoma. Eleven masses were malignant: there were five liposarcomas, two myxofibrosarcomas and one patient each with leiomyosarcoma, synovial sarcoma, sarcoma not otherwise specified (NOS) and soft tissue lymphoma. The largest lesion diameter ranged from 1.2 to 17.8 cm (median 6.3 cm) for the benign tumors and from 2.5 to 12.1 cm (median 7.8 cm) for the malignant tumors. Lesions were located in the forearm (5), upper leg (4), pelvis (3), knee (3), lower leg (3), and one each in the foot, axilla, upper arm, shoulder, and abdomen. The institutional review board approved the study protocol, and informed consent was obtained from all patients.

MR imaging

All patients underwent diffusion-weighted MR imaging as part of our standard MR protocol using a 1.5-T MR system (Philips Medical Systems, Best, The Netherlands) with a maximum gradient strength of 23 mT/m. All images were obtained with a surface coil. A diffusion-weighted spin echo sequence with peripheral pulse triggering (TR 2-RR, TE 70, flip angle 90°, field of view 200-300 mm, matrix size 51x128) was used with diffusion gradient strengths yielding 5 b-values ranging from 0 to 701 s/mm^2 (b=0, 176, 351, 526, and 701 seconds/mm^2). Acquisition time for the complete set of five b-values was on average 12 minutes. No respiratory triggering was used. Six slices

through the tumor were acquired with a slice thickness of 5 mm, and an interslice gap of 2.5 mm. Body parts containing the tumors were immobilized to prevent motion artifacts. Signal attenuation in each pixel is represented by:

$$SI/SI_0 = \exp(-b \times ADC) \qquad (1)$$

Where SI is the signal intensity in the pixel with the diffusion gradient, SI_0 is the signal intensity in the pixel without the diffusion gradient, b is the gradient factor, and ADC is the apparent diffusion coefficient.
Measurement of signal attenuation at different diffusion-sensitizing gradient strengths allows estimation of true diffusion coefficients and the perfusion fraction (1;10;11), using:

$$SI/SI_0 = (1 - f) \times \exp(-bD) + f \times \exp(-bD^*) \qquad (2)$$

Where SI is the signal intensity in the pixel with the diffusion gradient, SI_0 is the signal intensity in the pixel without the diffusion gradient, D and D^* are the true diffusion coefficient and the pseudodiffusion coefficient associated with perfusion, respectively, and f is the perfusion fraction (the fraction of the signal originating from perfusing spins). The biexponential variation of signal attenuation versus b-value is used to identify the presence of incoherent motion other than diffusion (perfusion). If there is contribution of perfusion, this effect is observed as a pseudodiffusion process. For large b-values, perfusion effects have been canceled out and D^* can be neglected. In contrast to this, at smaller values of b, signal attenuation reflects both diffusion and perfusion (1;12;13). This simple two-compartment model neglects exchanges between capillaries and the tissue, and differences in relaxation between these compartments (10).

Arbitrary-shaped regions of interest (ROIs) for data analysis were positioned in tumor, skeletal muscle, subcutaneous fat and bone marrow on the basis of the T2-weighted reference image (b=0 seconds/mm^2) and copied to all isotropic images of subsequent b-values. For the purpose of this study we assumed diffusion to be isotropic. When multiple tumor components (solid versus cystic) could be identified, measurements were taken in the solid components. Measurements of normal tissue were only obtained when there was a substantial amount of muscle, fat or bone marrow within the field of view. The mean signal intensities on five isotropic images

obtained with different b-values were used in Eq. (1) to calculate the ADC values, and in Eq. (2) to calculate D and f values by using a bi-exponential least-squares fit.

Differences in ADC values and true diffusion coefficients between malignant and benign soft tissue masses were evaluated using Student's *t* test. *P* values less than 0.05 were considered a statistically significant difference.

RESULTS

Due to breathing artifacts, evaluation of the measurements was not possible in one patient with a soft tissue lymphoma of the shoulder.

Muscle was evaluated in 19 patients, bone marrow in 14, subcutaneous fat in 17, benign soft tissue masses in 12 and malignant soft tissue tumors in 10 (Table 1). True diffusion coefficients of all soft tissue lesions combined, and of benign and malignant soft tissue tumors separately, were significantly higher than true diffusion coefficients of the surrounding tissues (*P < 0.05*) (Table 1).

The ADC's measured in normal tissue and tumors were higher than the perfusion-corrected true diffusion coefficients. This difference was significant for all tumors combined, for the malignant tumors, and for muscle and subcutaneous fat (Table 1). Perfusion fraction data are also listed in Table 1.

As shown in Table 1, true diffusion coefficients of benign soft tissue masses (mean ± standard error of the mean [S.E.M.] $1.71 \times 10^{-3} \pm 0.26$ mm^2/second) were significantly higher than true diffusion coefficients of malignant soft tissue tumors (mean ± S.E.M. 1.08×10^{-3} (0.23 mm^2/second) (*P < 0.05*) (Figure 1, 2).

The true diffusion coefficients of the individual soft tissue tumors with corresponding histology are presented in Table 2. The ADC values of benign soft tissue masses (mean ± S.E.M. $1.78 \times 10^{-3} \pm 0.24$ mm^2/second) were not significantly different from the ADC values of malignant soft tissue tumors (mean ± S.E.M. $1.30 \times 10^{-3} \pm 0.22$ mm^2/second) (*P > 0.05*).

Table I
ADC-values, true diffusion coefficients and perfusion fractions in soft tissue tumors

	ADC ($\times 10^{-3}$ mm^2/second)	True Diffusion Coefficient ($\times 10^{-3}$ mm^2/second)	Perfusion fraction
Subcutaneous fat (n= 17)	0.23 ± 0.04 *	0.18 ± 0.04	0.03 ± 0.006
Muscle (n=19)	1.08 ± 0.10 *	0.61 ± 0.11	0.23 ± 0.04
Bone marrow (n=14)	0.30 ± 0.08	0.27 ± 0.12	0.03 ± 0.008
All soft tissue lesions (n=22)	1.56 ± 0.17 *	1.42 ± 0.19	0.09 ± 0.02
Benign lesions (n=12)	1.78 ± 0.24 ⎫ N.S.	1.71 ± 0.26 ⎫ <0.05	0.07 ± 0.02 ⎫ N.S.
Malignant lesions (n=10)	1.30 ± 0.22 * ⎭	1.08 ± 0.23 ⎭	0.11 ± 0.02 ⎭

Numbers are the mean ± standard error of the mean

N.S. = not significant

* The ADC value was significantly higher than the true diffusion coefficient (*P < 0.05*)

Table 2

True diffusion coefficients of soft tissue tumors with corresponding histology.

Benign soft tissue masses	True Diffusion Coefficient (x 10^{-3} mm^2/second)
Myxoma	2.90
Synovial cyst	2.86
Hematoma	2.65
PVNS	2.55
Schwannoma	1.95
Schwannoma	1.36
Myositis	1.73
Ganglion	1.57
Vascular malformation	1.21
Leiomyoma	1.12
Fibromatosis	0.34
Fibromatosis	0.19

Malignant soft tissue tumors	True Diffusion Coefficient (x 10^{-3} mm^2/second)
Liposarcoma (myxoid and round cell, intermediate grade)	2.20
Liposarcoma (myxoid and round cell, intermediate grade)	1.88
Liposarcoma (well-differentiated sclerosing)	1.13
Liposarcoma (well-differentiated adipocytic)	0.25
Liposarcoma (well-differentiated adipocytic)	0.28
Myxofibrosarcoma (low-grade)	2.05
Myxofibrosarcoma (high-grade)	0.78
Leiomyosarcoma	0.83
Sarcoma NOS	0.73
Synovial sarcoma	0.66

DISCUSSION

Our results demonstrate significantly increased true diffusion in benign soft tissue masses compared to their malignant counterparts, whereas the ADC values between these groups are not significantly different. This difference can be explained by the contribution of perfusion to the ADC values. The two most important components of signal attenuation on diffusion-weighted MR images in soft tissue tumors are diffusion of water molecules in the extracellular space and perfusion (14;15). Perfusion fractions of malignant soft tissue tumors tend to be higher than that of the benign soft tissue masses (Table 1). Therefore, perfusion contributes more to ADC values in malignant soft tissue tumors than it does in benign soft tissue lesions. The impact of perfusion on

ADC values has been described in experiments with resected animal kidneys. Applying different flow rates through the isolated kidney resulted in true diffusion coefficients that remained the same, whereas ADC values increased with increasing flow rates (perfusion) (16).

The accuracy of this diffusion and perfusion parameter estimation by diffusion-weighted MR imaging was assessed by Pekar et al. (17). They reported on precise estimation of the true diffusion coefficient even with modest signal-to-noise ratios. However, perfusion fraction estimation is difficult, as the biexponential least-square fit method with curve stripping to refine a "starting guess" is prone to errors unless high signal-to-noise ratios are present (17). Therefore, the perfusion fraction we found may be subject to error variance, especially when the perfusion fractions are small (17). Estimation of the perfusion fraction in the more-vascularized malignant lesions will be more accurate than that in the less-vascularized benign lesions.

We obtained diffusion-weighted MR images with different diffusion-sensitizing gradient strengths (maximum b-value of 701 seconds/mm^2). In this way, true diffusion coefficients, corrected for the perfusion effect, could be estimated using Eq. (2). Le Bihan et al. reported that the transformation between perfusion and diffusion effect occurs at b-values in the 100-300 seconds/mm^2 range. In order to separate diffusion from perfusion effects, b-values of at least 500-800 s/mm^2 are needed (13). The size of the extracellular space is the most important component of the true diffusion measurement in soft tissue tumors. A larger or less restricted extracellular space, allowing spin dephasing and loss of signal on diffusion-weighted images, is the most likely explanation for the increased diffusion of most benign soft tissue tumors. Malignant soft tissue tumors tend to have lower true diffusion measurements due to increased tumor cell packing in the majority of the malignant soft tissue tumors, resulting in restriction of Brownian motion in the extracellular space. However, we realize that not all benign soft tissue tumors have a large extracellular space, and not all malignant soft tissue tumors are more cellular than benign soft tissue tumors. Moreover, we observed considerable variation in true diffusion values within the group of liposarcomas and between the high and low-grade myxofibrosarcoma (Table 2). A possible explanation may be related to the various histologic subtypes and variation in degree of differentiation of the tumor.

The two patients with benign lesions, demonstrating very low true diffusion coefficients similar to diffusion values of malignant soft tissue tumors, had aggressive fibromatosis. Histologically, aggressive fibromatosis consists of relatively uniform
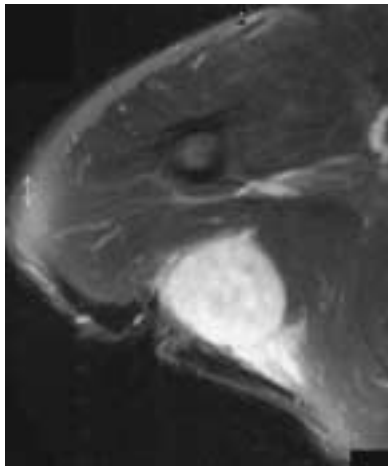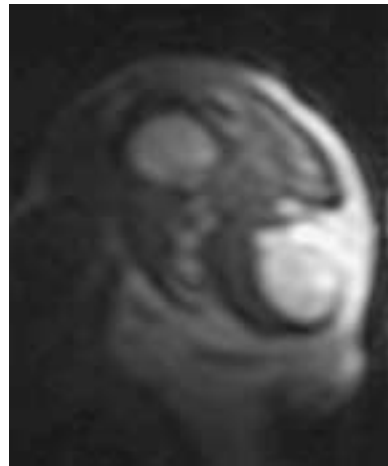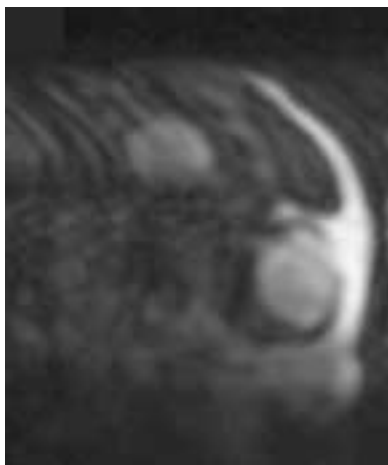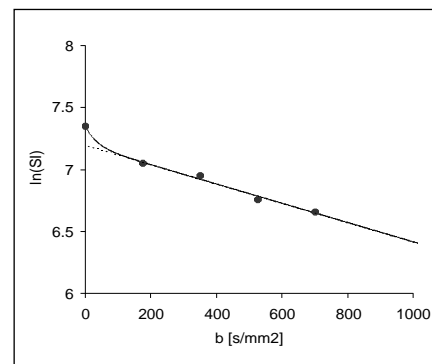
Figure 1a

Figure 1b

Figure 1c

Figure 1d

Figure 1

A 42-year-old man with a myxofibrosarcoma of the axilla.

a Axial T2-weighted MR image (TR 2968, TE 80) with fat saturation shows a high signal intensity soft tissue mass.

b Oblique diffusion-weighted MR image obtained with a b-value of 0 seconds/mm2 displays the lesion (arrowhead).

c Oblique diffusion-weighted MR images of the same slice obtained with a b-value of 701 seconds/mm2

d Corresponding graph of signal attenuation versus b-value of the soft tissue mass. The initial curved part of the graph indicates the effects of both diffusion and perfusion (perfusion fraction 0.14), according to the IVIM theory as proposed by Le Bihan (1). By increasing the gradient strength, and thus the b-value, the contribution of the perfusion to the diffusion measurement is cancelled out. This results in a straightening of the line. The slope of the straight line represents the true diffusion (true diffusion coefficient 0.78 x 10-3 mm2/second).

spindle-shaped cells surrounded and separated from each other by collagen fibers. However, fibrosarcoma is also composed of a relatively uniform population of spindle cells, demonstrating variable anaplasia. Fibrosarcoma is differentiated from aggressive fibromatosis by increased collagen and the absence of atypia in the latter, which is beyond the reach of diffusion-weighted MR imaging (18).

There have been few studies reporting on diffusion-weighted MR imaging in normal muscle, bone marrow or soft tissue tissues (9;19-22). The comparison of our results with existing reports is complicated by the differences in imaging sequences employed (9;17) and by the use of different and frequently low b-values (19;20). Diffusion values increase significantly with lower b-values, due in part to increased effect of perfusion at low b-values (1;10;23).

Several techniques have been used to obtain diffusion-weighted MR images (13). We used a peripheral pulse-triggered conventional spin-echo sequence that corrects for, or minimizes the effects of vascular pulsation on MR images in the extremities, and which was described previously as a successful sequence for diffusion measurements (22;24;25). The main disadvantage of the spin-echo sequence is the long acquisition time, and the subsequent increased sensitivity to motion artifacts. Faster imaging sequences, such as echo planar techniques, are available and have been used for diffusion measurements in human brain (10), hepatic lesions (11) and in the pelvis (21). In experiments with echo-planar imaging (EPI) of IVIM in the musculoskeletal system we encountered considerable chemical shift artifacts, as also reported by Baur et al. (15;19). Steady-state free precession (SSFP) techniques have also been used in the musculoskeletal system for diffusion-weighted MR imaging, with reported adequate image quality, signal-to-noise ratios and relatively short acquisition times (9;15;19). The main disadvantages of the SSFP technique are the difficulties in quantifying diffusion, T2-contamination and other confounding relaxation effects (15;26). Apparently, further studies are warranted to achieve faster diffusion-weighted spin-echo and/or EPI sequences with adequate image quality for diffusion measurements in the musculoskeletal system.

In contrast to Gd-DTPA-enhanced MR imaging, true diffusion measurements with diffusion-weighted MR imaging using high and low b-values can be used to separate the effects of small-vessel perfusion and extracelullar diffusion. The main disadvantage of contrast-enhanced MR imaging as compared to diffusion-weighted MR imaging is that the usually applied low molecular weight gadolinium chelates are distributed in the extracellular space, thus obscuring the separate effects of perfusion
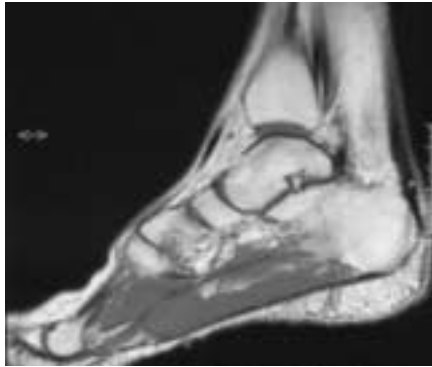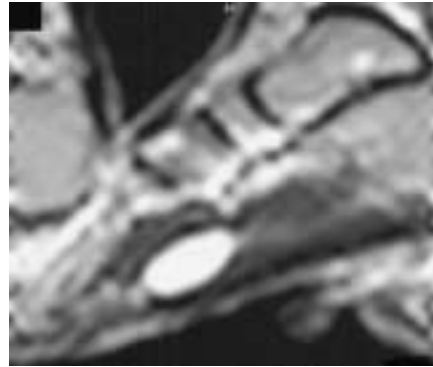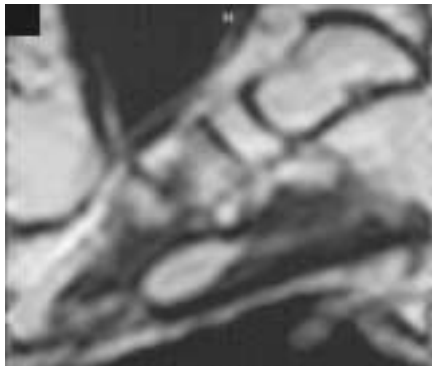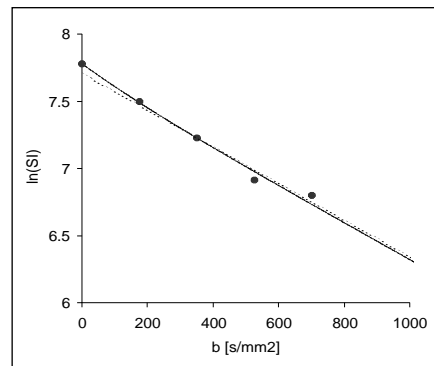
Figure 2a

Figure 2b

Figure 2c

Figure 2d

Figure 2

A 63-year-old female with a schwannoma of the foot.

a Sagittal T1-weighted MR image (TR 550, TE 7) exhibits a well-defined lesion with homogeneous signal intensity isointense to muscle (arrowhead).

b Sagittal diffusion-weighted image (TR 1846, TE 70) obtained with a b-value of 0 seconds/mm2

c Sagittal diffusion-weighted image (TR 1846, TE 70) of the same slice obtained with a b-value of 701 seconds/mm2. By increasing the diffusion gradient strength the signal intensity of the lesion is considerable reduced. Note that the diffusion-weighted MR images are slightly distorted due to infolding, however this did not effect the diffusion measurements.

d The initial part of the graph indicates both diffusion and perfusion effect (perfusion fraction 0.08). The slope of the fitted (dotted) line represents the true diffusion coefficient (true diffusion coefficient 1.36 x 10-3 mm2/second)

and diffusion (27;28). The measurement of the perfusion fraction in soft tissue tumors is difficult and less likely to provide clinically useful information. The true diffusion coefficient can be accurately estimated by the IVIM model and may play an important role in improved characterization of musculoskeletal tumors, and improved evaluation of tumor response to therapy. Recent work with animal models has demonstrated accurate differentiation between viable and necrotic tumor in osteogenic sarcoma by the use of diffusion-weighted MR imaging (7).

In conclusion, true diffusion measurements, which are corrected for the perfusion effect, has potential as a noninvasive parameter in the characterization of soft tissue masses, warranting further prospective studies with larger patient populations.

REFERENCES

1. Le Bihan D, Breton E, Lallemand D, Aubin ML, Vignaud J, Laval-Jeantet M. Separation of diffusion and perfusion in intravoxel incoherent motion MR imaging. Radiology 1988; 168:497-505.

2. Gonzalez RG, Schaefer PW, Buonanno FS, et al. Diffusion-weighted MR imaging: diagnostic accuracy in patients imaged within 6 hours of stroke symptom onset. Radiology 1999; 210:155-162.

3. Karonen JO, Liu Y, Vanninen RL, et al. Combined perfusion- and diffusion-weighted MR imaging in acute ischemic stroke during the 1st week: A longitudinal study. Radiology 2000; 217:886-894.

4. Marks MP, de Crespigny A, Lentz D, Enzmann DR, Albers GW, Moseley ME. Acute and chronic stroke: navigated spin-echo diffusion-weighted MR imaging. Radiology 1996; 199:403-408.

5. Tien RD, Felsberg GJ, Friedman H, Brown M, MacFall J. MR imaging of high-grade cerebral gliomas: value of diffusion-weighted echoplanar pulse sequences. AJR Am J Roentgenol 1994; 162:671-677.

6. Tsuruda JS, Chew WM, Moseley ME, Norman D. Diffusion-weighted MR imaging of the brain: value of differentiating between extraaxial cysts and epidermoid tumors. AJR Am J Roentgenol 1990; 155:1059-1065.

7. Lang P, Wendland MF, Saeed M, et al. Osteogenic sarcoma: noninvasive in vivo assessment of tumor necrosis with diffusion-weighted MR imaging. Radiology 1998; 206:227-235.

8. Maier CF, Paran Y, Bendel P, Rutt BK, Degani H. Quantitative diffusion imaging in implanted human breast tumors. Magn Reson Med 1997; 37:576-581.

9. Baur A, Stabler A, Bruning R, et al. Diffusion-weighted MR imaging of bone marrow: differentiation of benign versus pathologic compression fractures. Radiology 1998; 207:349-356.

10. Turner R, Le Bihan D, Maier J, Vavrek R, Hedges LK, Pekar J. Echo-planar imaging of intravoxel incoherent motion. Radiology 1990; 177:407-414.

11. Yamada I, Aung W, Himeno Y, Nakagawa T, Shibuya H. Diffusion coefficients in abdominal organs and hepatic lesions: evaluation with intravoxel incoherent motion echo-planar MR imaging. Radiology 1999; 210:617-623.

12. Le Bihan D, Turner R, Moonen CT, Pekar J. Imaging of diffusion and microcirculation with gradient sensitization: design, strategy, and significance. J Magn Reson Imaging 1991; 1:7-28.

13. Le Bihan D. Molecular diffusion nuclear magnetic resonance imaging. Magn Reson Q 1991; 7:1-30.

14. Latour LL, Svoboda K, Mitra PP, Sotak CH. Time-dependent diffusion of water in a biological model system. Proc Natl Acad Sci U S A 1994; 91:1229-1233.

15. Baur A, Reiser MF. Diffusion-weighted imaging of the musculoskeletal system in humans. Skeletal Radiol 2000; 29:555-562.

16. Pickens DR III, Jolgren DL, Lorenz CH, Creasy JL, Price RR. Magnetic resonance perfusion/diffusion imaging of the excised dog kidney. Invest Radiol 1992; 27:287-292.

17. Pekar J, Moonen CT, van Zijl PC. On the precision of diffusion/perfusion imaging by gradient sensitization. Magn Reson Med 1992; 23:122-129.

18. Scott SM, Reiman HM, Pritchard DJ, Ilstrup DM. Soft tissue fibrosarcoma. A clinicopathologic study of 132 cases. Cancer 1989; 64:925-931.

19. Baur A, Huber A, Arbogast S, et al. Diffusion-weighted imaging of tumor recurrencies and posttherapeutical soft-tissue changes in humans. Eur Radiol 2001; 11:828-833.

20. Morvan D. In vivo measurement of diffusion and pseudo-diffusion in skeletal muscle at rest and after exercise. Magn Reson Imaging 1995; 13:193-199.

21. Nonomura Y, Yasumoto M, Yoshimura R, et al. Relationship between bone marrow cellularity and apparent diffusion coefficient. J Magn Reson Imaging 2001; 13:757-760.

22. Ward R, Caruthers S, Yablon C, Blake M, DiMasi M, Eustace S. Analysis of diffusion changes in posttraumatic bone marrow using navigator-corrected diffusion gradients.
AJR Am J Roentgenol 2000; 174:731-734.

23. Melhem ER, Itoh R, Jones L, Barker PB. Diffusion tensor MR imaging of the brain: effect of diffusion weighting on trace and anisotropy measurements. AJNR Am J Neuroradiol 2000; 21:1813-1820.

24. Englander SA, Ulug AM, Brem R, Glickson JD, van Zijl PC. Diffusion imaging of human breast.
NMR Biomed 1997; 10:348-352.

25. Le Bihan D, Breton E, Lallemand D, Grenier P, Cabanis E, Laval-Jeantet M. MR imaging of intravoxel incoherent motions: application to diffusion and perfusion in neurologic disorders.
Radiology 1986; 161:401-407.

26. Le Bihan DJ. Differentiation of benign versus pathologic compression fractures with diffusion-weighted MR imaging: a closer step toward the "holy grail" of tissue characterization?
Radiology 1998; 207:305-307.

27. Delorme S, Knopp MV. Non-invasive vascular imaging: assessing tumour vascularity.
Eur Radiol 1998; 8:517-27.

28. Tofts PS, Brix G, Buckley DL, et al. Estimating kinetic parameters from dynamic contrast-enhanced T(1)- weighted MRI of a diffusable tracer: standardized quantities and symbols.
J Magn Reson Imaging 1999; 10:223-232.